A PERMEABILITY-POROSITY RELATIONSHIP FOR SURFACE DEPOSITION

G.J. WEIR AND S.P.WHITE

NZ Institute for Industrial Research and Development, Lower Hutt, NZ

SUMMARY – The changes to porosity and permeability resulting from surface deposition and early dissolution in an initial rhombohedral array of uniform spheres are calculated. Very rapid decreases of permeability result from early deposition, with 48% reduction predicted in permeability from 8% reduction in porosity. After deposition has caused about a 1% increase in the radii of the spherical array, relative permeability reductions vary approximately as the square of relative changes in porosity. These theoretical results are matched with experimental data of Ioti et *al.*, and shown to be satisfactory in some cases, but for others, a more complex model of the porous medium is needed.

1 INTRODUCTION

Within the earth, pore sizes of 10 nm to 1000 nm (10^{-6} m) frequently occur. Deposition in such pores can be viewed as beneficial when ore deposits form, or as detrimental, when silica blocks geothermal flows to wells. On the very large scale, calcite deposition (flowstone) in caves, or dams (gours) forming when water flows over the outflow of subterannean pools, are examples of pore sizes of many metres. Consequently, deposition can be viewed as microscopic or macroscopic [1] phenomena.

The primary motivation for this paper is to quantify effects from surface deposition in geothermal fields. We ignore non-surface deposition. We shall assume that flow within the pores is laminar. and that diffusion is not rate controlling. Our justification for the last assumption is that if 10^{-7} m/s is a typical Darcy velocity, 10^{-6} m a typical pore radius, 10^{-1} a typical porosity, and 10^{-9} m^2/s a typical diffusivity for a depositing molecule, then the time for fluid to pass through a pore is about 1 s, but the time for concentration gradients to reduce significantly within a pore is only about 10^{-3} s.

Deposition is therefore determined largely fiom the geometry of the porous medium. If mass deposition is occurring at a rate D per unit area of available solid surface, then growth occurs normal to *such* surfaces at the rate,

$$\frac{d\xi}{dt} = \frac{D}{\rho_d} \qquad (1)$$

where ξ denotes the position of the surface, ρ_d is the density of the deposited layer, and D depends on concentrations and temperature. We shall assume that (1)holds in the remainder of this paper.

The assumption in (1) is a severe restriction on variations on porosity and permeability resulting from deposition. In particular, since porosity will decrease monotonically with the amount of deposition, and permeability will also vary monotonically with the amount of deposition,

$$k = k_0 f(\phi, \phi_0) \qquad (2)$$

where k is permeability, k_0 initial permeability, ϕ porosity. ϕ_0 initial porosity, and f is some non-dimensional function. which depends on the structure of the porous media. but is independent of temperature and pressure.

In deriving (2), we have assumed that once a pore has been cut off, so that flow no longer occurs through that pore. thar subsequent deposition is minimal. Once a pore has cut off, the rate of deposition will alter, since fluid is no longer available to replenish deposited components, and concentrations will differ locally fiom that in open pores. However, if depositing concentrations are typically small, such as say 200 ppm, then the change in linear dimensions within the pore after cut off is less than .01 %, so that deposition can be assumed to stop instantaneously with cut off. Then (2) should hold.

For the numerical modelling in the next section, we need to determine the function f in (2). This can be done either from using experimental data, or from developing a simple model to predict f. We shall attempt to derive f from a simple model. Note that this only requires that we know the variation of permeability to within a multiplicative constant.

Such models need to predict the general behaviour found experimentally. Graham [5]has shown that during deposition, porosity tends to a critical non-zero porosity, ϕ_c, while permeability tends to zero, as

$$k \sim (\phi - \phi_c)^{1.8} \qquad (3)$$

Another experimental finding [14] is that small changes in porosity (about 8%) can significantly reduce permeability (by about 96%). This seems to contradict (3), which predicts

much smaller changes in permeability. One aim of this paper is to attempt to resolve this apparent contradiction.

Changes in permeability and porosity resulting from changes in pressure appear to differ significantly from those occurring from deposition. During compression, permeability apparently does not tend to zero, by to some non-zero value [17], possibly because it is effectively impossible to close off all pathways from compression. For this reason, we shall not consider compression further in this paper.

We begin by considering the slow laminar passage of fluid through a variable (though periodic) porous media. A force balance through a cross-section of the porous medium gives

$$\frac{d}{dy}\int pdA = \int \tau dL \sim -\frac{\mu L^2 u}{A} \tag{4}$$

where p is pressure on the cross-section, A area, τ viscous shear stress, L a length scale along solid surfaces in the cross-section, μ viscosity, u is the mean fluid speed through the cross-section, and y distance perpendicular to the cross-section. Pressure will vary across any cross-section. We assume that mean pressure P at position y, satisfying

$$\int pdA = \overline{A}P \tag{5}$$

has phyical significance. In (5), $\overline{A}$ denotes the average area over height y,

$$\overline{A} = \frac{1}{Y}\int_0^Y A dy \tag{6}$$

Since in steady flow, the volumetric flow of fluid uA is constant, it is possible to integrate the changes in pressure P over a finite length, and hence to derive an apparent Darcy Law, in which permeability varies as

$$k \sim \frac{\overline{A}}{A_T}\frac{1}{\overline{L^2 A^{-2}}} \tag{7}$$

where A_T is the total area considered. For equal radius vertical cylinders, the ratio of the left hand side to the right hand side in (7) is 1/2, and 1/3 for vertical fractures of constant aperture.

The porosity is

$$\phi = \frac{\overline{A}}{A_T} \tag{8}$$

Deposition removes chemicals from the liquid phase, and so a sink term is needed to describe this process. The form of this sink term is assumed to be

$$\frac{dC}{dt} = -Kh\frac{A}{V} \tag{9}$$

where A/V is the local exposed solid area per unit pore volume, h is a function of temperature, and the constant K depends on the nature of the fluid and solid-surface. Locally, the mean value of the ratio A/V equals L/A, but we do not have an exact expression for this ratio in terms of permeability k and porosity ϕ. However, a related expression exists in (7) for the the mean value of the square of L/A. From (7) and (9), we shall assume that the sink term in the fluid obeys

$$\frac{dC}{dt} = -Kh\sqrt{\frac{\theta\phi}{k}} \tag{10}$$

where θ is a constant of the order of unity.

The aim of the next section is to evaluate porosity and permeability changes in a simple geometry, using (7) and (8). A related approach has been made recently by Lu et al [8] who analysed water rise due to surface tension and gravity through close packed arrays of spheres of uniform radius. Much earlier, an extensive investigation of the permeability and porosity of systematically packed spheres was conducted by Graton and Fraser [6].

2 Rhombohedral Packing of Spheres

We begin by assuming an initial rhombohedral packing of uniform spheres of radius R. From Fig. 1, this can be imagined as lines of spheres with their centres separated by $2R$ in the x direction; the lines being separated by $\sqrt{3}R$ in the y direction; and horizontal planes separated by $2\sqrt{2/3}R$ in the z direction, since the centres of adjacent spheres form tetrahedra. One horizontal layer of spheres is shown as heavy circles, and the layer above by light circles. (There are two [6] rhombohedral packings, which differ by the upper plane of spheres being rotated by about 109° 28' within its own plane. We do not consider both cases in this paper.)

The porosity of this structure is [2] $(4\sqrt{2} - 4\pi/3)/4\sqrt{2}$, or about 26%. This is rather large for many natural materials. for which a porosity of about 10% may be more usual. Nevertheless, we shall consider deposition in this structure. Let ξ be the thickness of deposit which has formed on the spherical surfaces. Since deposits *grow* perpendicular to surfaces, the exposed spherical surfaces preserve their shape.

The maximum thickness of deposit ξ_m before permeability is destroyed follows from Fig. 1,

$$\frac{\xi_m}{R} = \frac{(2-\sqrt{3})}{\sqrt{3}} \sim .1547 \tag{11}$$

since permeability fails when the coallescing inward growing surfaces meet at the centre of the in-circle in the equilaterial triangle formed from joining adjacent spherical centres in Fig. 1.

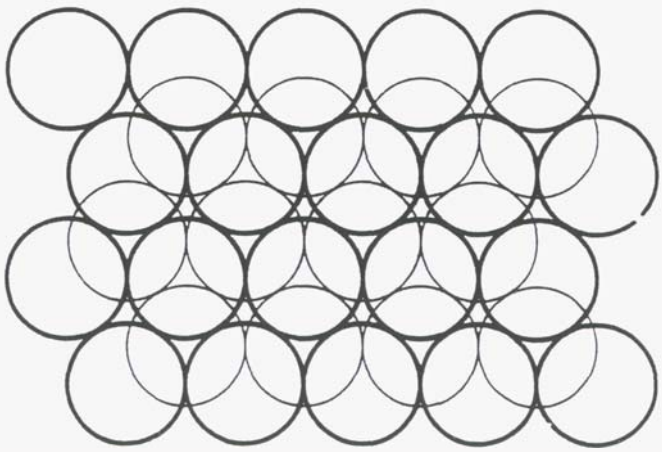

Figure 1. Rhombohedral Packing of Spheres.

Before deposition begins, each sphere contacts twelve other spheres. After deposition begins, the porosity can be determined fromcalculating the volume of *each* sphere (with radius $R+\xi$), and subtracting (half of) the twelve volumes of intersection. Since the unit replicating volume is $4\sqrt{2}R^3$, the porosity (ϕ) is found to be

$$\phi = 1 - \frac{\pi}{3\sqrt{2}R^3}\left[(R+\xi)^3 - 3\xi^2(3R+2\xi)\right] \qquad (12)$$

From (11) and (12), the residual porosity at zero permeability is about 0.0359.

Before permeability fails, fluid can move up through the voids shown in Fig.1, being constrained initially to one channel, but on moving further up through the array of spheres, the fluid path has a choice of at least six nearby channels between the spheres in the the upper layer of spheres. The complexity of these channels is emphasised by Graton and Fraser ([6], p. 857).

The change in porosity as a function of the normalised change in radius ξ/R is relatively gradual, but the change in permeability is very rapid. For example, a 48% decrease in permeability results from an 8% decrease in porosity. However, after an increase in radius of about 1%, k decreases much slower. This change in behaviour can be interpreted in two ways. Figures 2 and 3 plot normalised permeability (k_n) as a function of normalised porosity (ϕ_n), where

$$k_n = \frac{k}{k_0} \qquad (13)$$

$$\phi_n = \frac{\phi - \phi_c}{\phi_0 - \phi_c} \qquad (14)$$

The discrete solid dots in Figs. 2 and 3 are theoretical values obtained using (7)and (8). The lower continuous curve in Fig. 2 is $k_n = .256\phi_n^{58.3}$, and fits the early decreases in permeability. The middle continuous curve in Fig. 2 is $k_n = .744\phi_n^{2.18}$, and fits the late decreases in porosity. The upper continuous curve equals the sum of the lower and middle curves, showing that the theoretical normalised permeability values *can* be fitted by a rapid initial decrease, plus a more gradual and approximately quadratic decrease thereafter. However, the late time behaviour was also fitted adequately by $k_n = .753\phi_n^{1.9}$, showing that the exponent connecting k_n to ϕ_n is about 2, depending on how the data points are weighted.

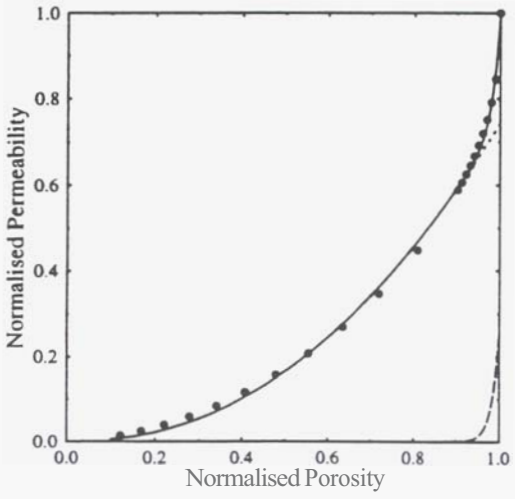

Figure 2. Normalised permeability versus normalised porosity.

The other way of interpretation is shown in Fig. 3, which draws a continuous *curve* approximately through the calculated points. The equation of this empirical continuous curve is

$$k_n = 1 - \left(1 - \phi_n^{1.58}\right)^{0.460} \qquad (15)$$

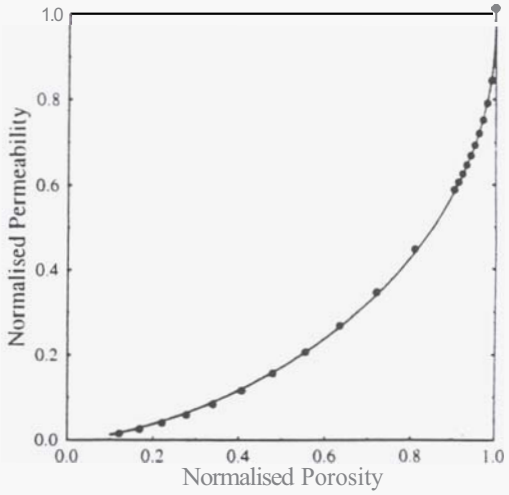

Figure 3. Normalised permeability versus normalised porosity.

The numerical evaluation of permeability according to (7) in a regular array of uniform spheres has the advantage that as the cross-sectional areas decrease from deposition, the mean value of L^2A^{-2} is likely to diverge to infinity, and so k can approach zero for a non-zero value of porosity. This property is not present in models in which the averages in (7) are estimated, as in Kozeny-Carmen formulae [4], since then permeability varies essentially as the cube power of porosity. (For planes, a cube power also arises, whereas for cylinders, a quadratic power is obtained.)

The plot in Figs. 2 and 3 has the property that very large decreases in permeability result from quite small (initial) changes in porosity, and also that k varies roughly as the second power of changes in ϕ. Since these properties are consistent with the experimental findings of Vaughan [14] and Graham [5], we have used the relationship in (15) for the following numerical examples.

3 COMPARISON WITH EXPERIMENT

The porous media model used in this work is similar to the porous columns used in [7]. In this work Itoi *et al.* conducted a number of experiments to investigate precipitation from fluids saturated with SiO_2. While there are some problems interpreting the chemistry of these experiments they provide an excellent source of data for verifying the model developed in this paper. In these experiments a sample of fluid supersaturated in SiO_2 (taken from the Otake geothermal field) is passed through a column packed with aluminium beads. The pressure difference between the ends of the tube is kept constant while the flow rate through the tube and pressure along the tube are measured. At the completion of the experiment

samples of the beads from different points along the tube are weighed to determine the mass of silica scale deposited on the beads. Itoi *et al.* present measurements of specific deposit (the ratio of scale mass to bead mass) and from this porosity changes may be calculated. Physical parameters associated with these calculations are taken mainly from [9] and are reproduced in Table 1.

Supersaturation	C_{inlet}-C_s	=	4.42 ppm
Column temperature	T	=	90°C
Initial porosity	ϕ_0	=	.4
Density of beads	ρ_r	=	3620 kg/m^3
Density of deposited silica	ρ_s	=	2040 kg/m^3
Porosity of silica	ϕ_s	=	0.932
Reaction rate coefficient	$k^- \frac{A}{M}$	=	0.6 s^{-1}

Table 1. Data used to match run 5 of Itoi *et al.*.

In Figure 4 we present two theoretical curves, one of these uses the theoretical value of $\phi_c = .04$ and the second (lower) uses a value of $\phi_c = .2$ which provides a better match to the data. Also presented in this figure is experimental data taken from runs 1-6 of Itoi *et al.*. This figure shows the initial rapid decrease in permeability for small amounts of deposition followed by much slower changes as seen in the experimental data.

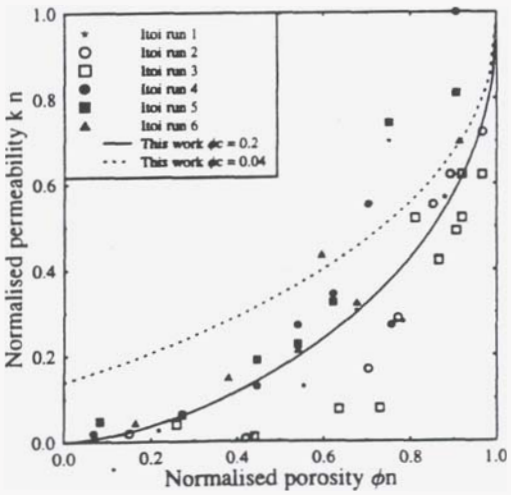

Figure 4. Comparison between Itoi *et al.* experimental data and (15).

We have also simulated this experiment using a modified version of the TOUGH2 simulator [11]. This program has been modified by White [16] to include the transport of reacting chemicals and makes it possible to calculate the pressure drop and deposition along the porous column. We have assumed Darcy flow in the column for these calculations and as pointed out in, [7] this may not be justified, particularly at early times. In Fig. 5 we present the calculated and measured pressures and in Fig. 6 the calculated and measured specific deposits for run 5 of [7].

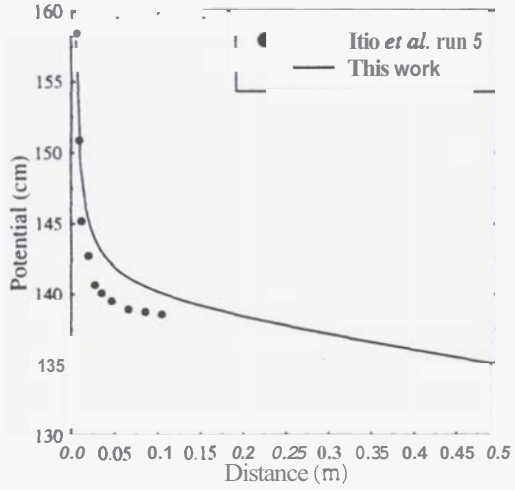

Figure 5. Theoretical and experimental pressure.

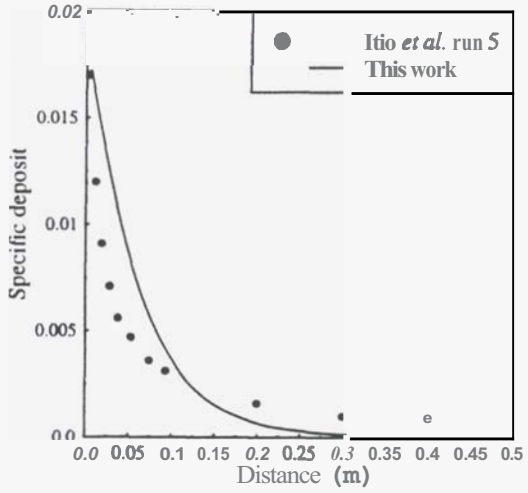

Figure 6. Theoretical and experimental specific deposit.

In order to model these experiments we require a rate law that allows us to calculate the deposition rate from solution. We have chosen to use the rate law suggested by Rimstidt and Barnes [12]

$$\frac{dC}{dt} = -k^- \frac{A}{M}(C - C_s) \qquad (16)$$

Here $\frac{A}{M}$ is the ratio of surface area available for precipitation to mass of water, k^- is the rate constant, C is the silicic acid concentration and C_s is the saturation concentration. k^- as a function of temperature is given by an Arrhenius law $\log k^- = -0.707 - 2589/T_k$ where T_k is the temperature in Kelvin. Malate and O'Sullivan [9] found that using the rate constant given in [12] leads to a very poor match to the experimental results in [7] and they have obtained a different value which matches the experimental results quite well. Our results agree with those of Malate and O'Sullivan and we have adopted a value of the rate constant similar to their value.

The permeability-porosity relationship derived in this paper were also used to duplicate another set of experimental data,

that determined by Moore *et al.* [10]. In a series of experiments, distilled water was passed down a temperature gradient through cylinders of granite. Temperatures at the outside of the cylinders were held in the range 80–100°C and the centre was held in the range 250–300°C. The change in flow rate was measured for a period of between one and three weeks and from this a change in permeability was determined. The model of a porous media used to derive the relationship between porosity and permeability given in (15) is unlikely to be correct for the granites of the experiments of Moore *et al.* [10] where permeability is most probably provided by micro-fractures and pipes formed by the intersection of micro-fractures. Nevertheless we felt it worthwhile to investigate how well the expression given in (15) would match experimental results from granite.

The rate equation for quartz precipitation is assumed to have the form [13]

$$\frac{dC}{dt} = \frac{A}{V} k_{25} \exp\left(\frac{-E_a}{R}\left(\frac{1}{T} - \frac{1}{298.15}\right)\right)\left(1 - \frac{\{SiO_2\}}{K_{SiO_2}}\right) \quad (17)$$

where k_{25} is the reaction rate constant at 25° C and we have assumed an Arrhenius equation for temperature dependence. E_a is the activation energy; $\frac{A}{V}$ the area over which the reaction occurs per unit volume of fluid; T the temperature in ° K; R the gas constant; $\{SiO_2\}$ the activity of aqueous SiO_2 and K_{SiO_2} the equilibrium constant for the dissolution of quartz reaction. Choice of $\frac{A}{V}$ is difficult; theoretical considerations suggest $\frac{A}{V} = \sqrt{\frac{\theta\phi}{\chi}}$ where θ is of the order of unity. This leads to values of $\frac{A}{V}$ in the range 3.5×10^7 - 1.1×10^8 m^{-1} for the experiments of Moore *et al.* considered here. In a recent paper, Bernabé [3] has simulated the transport properties of networks of cracks and pores. From this work, a figure in the range 1.2×10^6 - 1×10^7 m^{-1} is appropriate. We have found that a value of 6.5×10^3 provides a good match with run b250-1 of Moore *et al.*. We see from Fig. 7 that the match to experiment is quite good. The match with run b300 is not very good and there seem to be two mechanisms operating to provide permeability. Fig. 8 shows two matches to the permeability changes for run b300. We have chosen two values of $\frac{A}{V}$ to match the early and late time behaviour as it was not possible to match the whole time range. At early times there is a very rapid reduction in permeability and this is matched by a value of $\frac{A}{V}$ of 1.0×10^5 while at later times a value of 5.0×10^3 is more appropriate. The late time value is similar to that found for run b250-1.

It is interesting that the theoretical values of $k_{25}\frac{A}{V}$ in (17) are about three orders of magnitude too large for the the experimental data of Moore *et al.*. Possibly the reactions occur at a much slower rate! within rock than in the idealised laboratory situation used to determine the rate constant in (17), or else the flow is occurring mainly in a few large pores, for which the ratio A/V is much smaller than for the rock as a whole

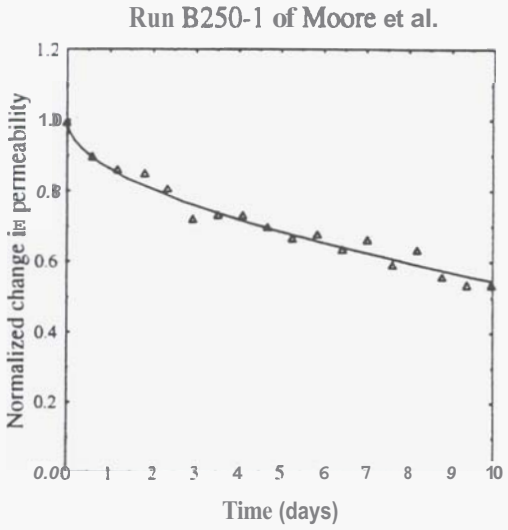

Figure 7. Match with run b250-1 of Moore *et al.*

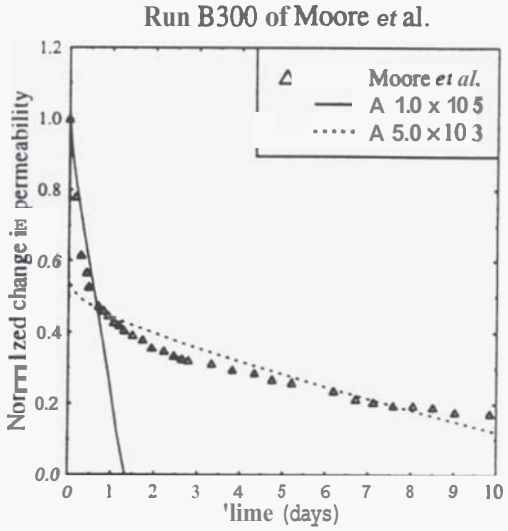

Figure 8. Match with run b300 of Moore *et al.*

4 CONCLUSIONS

The main new results contained in this paper are :

- Theoretical calculations of permeability and porosity changes resulting from deposition or dissolution in an initial rhombohedral array of uniform spheres;
- Determination of empirical relationships connecting changes in permeability and porosity resulting from deposition or dissolution in this initial array of uniform spheres;
- Discovery of a late time approximately quadratic dependence between relative changes in permeability and porosity, but preceded by a very rapid early reduction in permeability;

- There was no definite power relationship between normalised permeabilities and porosities for deposition in this late time behaviour, with values from 1.9 to 2.2 being suggested;
- An approximately fourth power relationship between permeability and porosity for initial dissolution;
- The permeability versus porosity relationship derived in this paper matches experimental results for a porous column formed from beads. The very rapid initial change in permeability predicted by (15) is observed in the experimental data of Otoi.
- For more complex structures, such as some granites, (15) did not describe the late time behaviour resulting from deposition, for which a more complex porous media model will be needed.

Acknowledgements.

The authors acknowledge the assistance of Peter McGavin in preparing some of the figures.

References

1 Barber, M.N. and Singleton, D., Travelling Waves in Phase Field Models of Solidification, J. *Austral.* Math. *Soc., Ser. B*, 36, 325 - 371, 1994.

2 Bear, J., Dynamics of *fluids* in *porous* media, p. 46, American Elsevier, 1972.

3 Bernabé Y., The transport properties of networks of cracks and pores, *J. Geoph. Res.*, 100, B3, 4231-4241.

4 Fair, G.M. and Hatch, L.P., Fundamental Factors Governing the Streamline Flow of Water through Sand, Jour. *Amer. Water Works Assoc.*, Vol XXV, 1551 - 1565, 1933.

5 Graham, R.A., A quantitative determination of microstructure on gas permeability of UO_2 and Ni sintered bodies, *M.S. thesis*, Uni. of Fla., Gainesville, 1973.

6 Graton, L.C. and Fraser, H.J., Systematic packing of spheres with particular relation to porosity and permeability, *J.* Gwl., 8, (43), 785 - 909, 1935.

7 Itoi, R., Maekawa, H., Fukuda M., Jinno, K., Hatanaka, K., Yokoyama, T., Shimizu, S., Experimental Study on the silica deposition in a porous medium, *Trans. Geoth.* Resour. Coun., 8, 301-304, 1984.

8 Lu, T.X., Nielsen, D.R. and Biggar, J.W., Water movement in glass bead porous media 3. Theoretical analyses of capillary rise into initially dry media, Water *Resour. Res.*, 31, (1), 11-18, January 1995.

9 Malate, R.C.M., O'Sullivan, M.J., Mathematical modelling of silica deposition in a porous medium, *Geothermics*, 21, (3), 377-400, 1992.

10 Moore, D.E., Morrow, C.A., Byerlee, J.D., Chemical reactions accompanying fluid flow through granite held in a temperature gradient, Geochim. et Cosmochim. Acta, 47, 445-453, 1983.

11 Pruess, K., TOUGH2 - A general-purpose numerical simulator for multiphase fluid and heat flow, Rep. *LBL-29400-4645*, Lawrence Berkeley Lab., Berkeley, Calif., 1991.

12 Rimstidt, J.D., Barnes, H.L., The kinetics of silica-water reactions, Geochim. et Cosmochim. Acta, 44, 1683-1699, 1980.

13 Steefel, C.I., Lasaga, A.C. (1994) A coupled model for transport of multiple species and kinetic precipitation/dissolution reactions with application to reactive flow in single phase hydrothermal systems. Amer J. *Sci.* 249, 529-592 May 1994.

14 Vaughan, P.J., Analysis of permeability reduction during flow of heated, aqueous fluid through Westerly Granite, paper presented at International Symposium on Coupled Processes Affecting the Performance of a Nuclear Waste Repository, *US Dept of Energy*, Berkeley, Calif., Sept. 18 - 20, 1985.

15 Verma, A. and Pruess, K., Thermohydrological Conditions and *Silica* Redistribution Near High-Level Nuclear Wastes Emplaced in Saturated Geological Formations, *J. Geophys. Res.*, 93, 1159 - 1173, 1988.

16 White, S.P., Multiphase nonisothermal transport of systems of reacting *chemicals*, *Water Resour. Res.*, 31, 1761-1772, 1995.

17 Wyble, D.O., Effect of applied pressure on conductivity, porosity and permeability of sandstones, *Trans. Soc.* Pet. *Eng. AIME*, 213, 430 - 432, 1958.